JOURNAL OF VIROLOGY, Feb. 2005, p. 2274–2286 Vol. 79, No. 4
0022-538X/05/$08.00+0 doi:10.1128/JVI.79.4.2274–2286.2005

Expression Profiling of Human Hepatoma Cells Reveals Global Repression of Genes Involved in Cell Proliferation, Growth, and Apoptosis upon Infection with Parvovirus H-1†

Jianhong Li,[1,2] Ekkehard Werner,[2] Manfred Hergenhahn,[3] Rémy Poirey,[2] Zuyu Luo,[1] Jean Rommelaere,[2] and Jean-Claude Jauniaux[2]*

Department of Physiology and Biophysics, Fudan University, Shanghai, People's Republic of China,[1] and Tumor Virology Division F010 and INSERM Unité 375[2] and Genetic Alterations in Carcinogenesis Division C040,[3] Deutsches Krebsforschungszentrum, Heidelberg, Germany

Received 8 June 2004/Accepted 23 September 2004

Autonomous parvoviruses are characterized by their stringent dependency on host cell S phase and their cytopathic effects on neoplastic cells. To better understand the interactions between the virus and its host cell, we used oligonucleotide arrays that carry more than 19,000 unique human gene sequences to profile the gene expression of the human hepatocellular carcinoma cell line QGY-7703 at two time points after parvovirus H-1 infection. At the 6-h time point, a single gene was differentially expressed with a >2.5-fold change. At 12 h, 105 distinct genes were differentially expressed in virus-infected cells compared to mock-treated cells, with 93% of these genes being down-regulated. These repressed genes clustered mainly into classes involved in transcriptional regulation, signal transduction, immune and stress response, and apoptosis, as exemplified by genes encoding the transcription factors Myc, Jun, Fos, Ids, and CEBPs. Quantitative real-time reverse transcription-PCR analysis on selected genes validated the array data and allowed the changes in cellular gene expression to be correlated with the accumulation of viral transcripts and NS1 protein. Western blot analysis of several cellular proteins supported the array results and substantiated the evidence given by these and other data to suggest that the H-1 virus kills QGY-7703 cells by a nonapoptotic process. The promoter regions of most of the differentially expressed genes analyzed fail to harbor any motif for sequence-specific binding of NS1, suggesting that direct binding of NS1 to cellular promoters may not participate in the modulation of cellular gene expression in H-1 virus-infected cells.

Autonomous parvoviruses are small, nonenveloped, linear single-strand DNA viruses. Their 5-kb-long genome consists of two overlapping transcription units. An early promoter, P4, directs the expression of nonstructural proteins NS1 and NS2, and a late promoter, P38, controls the expression of capsid proteins VP1 and VP2 (12). Owing to their low genetic complexity, parvoviruses are tightly dependent on cellular factors that are expressed as a function of proliferation and differentiation in order to complete their life cycle (53, 60). Parvoviruses are incapable of inducing quiescent cells to enter S phase (66), and infection remains cryptic until host cells start a round of genomic DNA replication on their own. Once the appropriate cellular conditions are met, the virus starts its replication at the G_1/S transition and a lytic or even productive infection can ensue (12, 22), during which the infected cells get blocked in S/G_2 phase and eventually die (48, 53). The tight dependence of parvovirus replication on S-phase-associated factors accounts, in part, for the tissue specificity, oncotropism, and oncolytic activity of parvoviruses (55). In particular, MVMp and the closely related H-1 virus were found to replicate and exert cytopathic effects in a variety of transformed or tumor-derived cells while sparing their normal counterparts in vitro. In vivo, these viruses may prevent tumors from appearing or cause the repression of established tumors, making them candidates for vectors in cancer therapy (9).

The molecular mechanisms underlying parvovirus-host cell interactions were the objects of a number of recent studies. On the viral side, the nonstructural proteins NS1 and NS2 are key regulators of the virus life cycle. NS1 is a multifunctional protein that is endowed with a transcriptional function targeted to parvoviral but also heterologous promoters (18, 31, 54, 67), and with enzymatic (ATPase, helicase [69], and site-specific nickase [44]) and site-specific DNA binding properties (10). NS1 thus plays critical roles during parvovirus replication and gene expression, starting from the earlier stages of the viral life cycle. NS2 has more elusive functions and appears to be particularly important in certain cells for capsid assembly and release of progeny viruses (11, 16). The viral effector of cytotoxicity has been assigned mainly to the nonstructural protein NS1 (6, 31), though other viral products may also be involved (4, 32). Completion of the viral life cycle requires the assistance of various cellular molecules; some of these have been identified, including transcription factors, cofactors, and other nuclear proteins. CyclinA (2), parvovirus initiation factor (PIF) (8), and two members of the protein kinase C (PKCλ/η) family play distinct roles in virus replication (28, 45). The transcription factors E2F (15) and SP1 (27), the transcription coactivator CBP (47), and the basal transcriptional factors TBP and TFIIA(α/β) (36) help NS1 to *trans*-regulate target promoters

* Corresponding author. Mailing address: Applied Tumor Virology, Abteilung F010 and INSERM U375, Deutsches Krebsforschungszentrum, Postfach 101949, D-69009 Heidelberg, Germany. Phone: 49 (0)6221 42 4971. Fax: 49 (0)6221 4252 4971. E-mail: j.jauniaux@dkfz.de.

† In memoriam: we are saddened by the death of Manfred Hergenhahn, who died suddenly on 13 May 2004.

through direct or indirect interactions with this protein. CREB and the Ets family of transcription factors (19, 50) may also participate in the regulation of viral promoter. SGT (13) and SMN (72) are partners of NS1. Members of the 14-3-3 protein family (5) and the nuclear export receptor Crm1 (3) interact with NS2.

The investigation of the impact of parvovirus infection on cellular processes at the molecular level is still in its infancy. Virus infection was reported to cause down-regulation of MYC expression (52) and release of heat shock protein 72 (41), and phosphorylation of distinct cellular proteins was also observed upon NS1 expression (1). In order to gain insight into the global changes in cellular gene expression occurring in cells at early times after exposure to parvovirus H-1, we applied Affymetrix oligonucleotide microarray technology. Chips carrying 19,000 unique human gene sequences were used to profile gene expression in the human hepatocellular carcinoma cell line QGY-7703, infected or not infected with the wild-type H-1 virus. This cell is highly susceptible to H-1-induced cell killing and produces progeny viruses (21, 65). In vitro infection of QGY-7703 cells with the H-1 virus strongly represses their ability to form both colonies in soft agar and tumors in nude mice (71). Furthermore, in vivo infection with the H-1 virus inhibits the development of established QGY-7703-derived tumors in animals bearing these neoplastic lesions (58). This system therefore appears to be suitable to explore the mechanism of parvovirus oncosuppression at the molecular level. By comparing the mRNA levels of H-1 virus-infected cells with those of mock-treated synchronized cells, we identified distinct genes which show altered expression upon H-1 virus infection and provide new clues to the understanding of parvovirus-host interactions.

MATERIALS AND METHODS

Cell culture and synchronization. The established human hepatocellular carcinoma cell line QGY-7703 was obtained from the Laboratory of Molecular Cell Biology, Fudan University (Shanghai, People's Republic of China). Cells were cultured in RPMI 1640 medium (Sigma) supplemented with 10% fetal calf serum, 100 U of penicillin/ml, 100 U of streptomycin/ml, and 2 mM glutamine in a 5% CO_2 atmosphere at 37°C. Cells were tested by PCR to exclude mycoplasma contamination. For synchronization, the cells were seeded and incubated under the conditions mentioned above for 22 h. The medium was then replaced with fresh medium containing 400 μM mimosine (Sigma), and cultures were further incubated for 18 h, resulting in cell arrest in late G_1 phase. Cells were released from the mimosine treatment by washing cultures twice with fresh medium and further incubating them in normal medium. Culture aliquots were withdrawn and subjected to FACScan analysis to follow up the progress of cell cycle and determine the extent of synchronization.

Virus production and infection. Wild-type H-1 virus was propagated in NBK324 cells, purified on iodixanol gradient as previously described (70), and titrated by plaque assay using NB324K as indicator cells. The purity of the virus stock was analyzed by silver staining and Western blot analysis using a rabbit antiserum directed against a recombinant VP2 polypeptide that is shared by VP1, VP2, and VP3 (26). The ratio of full to empty virions in the virus stock was determined by electron microscope analysis. Cells to be infected were cultured as described above and infected at a multiplicity of infection (MOI) of 10 PFU per cell, or buffer (mock)-treated for 1 h in the presence of mimosine. After release from drug treatment, cells were harvested at different time points and subjected to experimental analyses. The experimental scheme used is illustrated in Fig. 1.

FACScan analysis. Synchronized, virus-infected, and mock (buffer)-treated cells were detached from dishes with trypsin (Gibco) and collected by centrifugation. The cell pellets were washed with phosphate-buffered saline (PBS) once and resuspended in 0.5 ml of PBS, followed by fixation in cold 75% ethanol and storage at 4°C. Before FACScan analysis, cells were washed with PBS, stained with 0.5 ml of PI solution (0.02 mg of propidium iodide/ml, 2 mg of RNase A/ml, 0.1% Triton X-100) at room temperature in the dark for 30 min. Fluorescence was measured from 10,000 events for each sample by using FACScan (BD Biosciences) and analyzed by using Cell Quest Software (BD Biosciences).

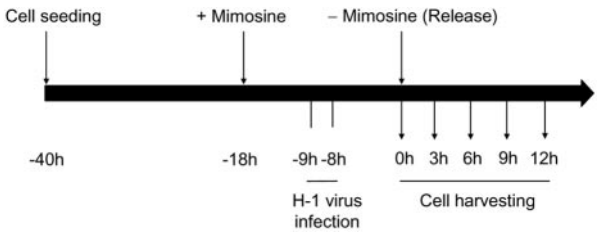

FIG. 1. Experimental scheme. QGY-7703 cells were cultured in minimal medium for 22 h after seeding. Medium was replaced with fresh medium containing mimosine (400 μM) and cells were further incubated for 18 h, during which time they were infected with the H-1 virus at a MOI of 10 PFU/cell for 1 h in the presence of mimosine. Cells were harvested at different time points after release from drug and subjected to analysis.

Immunofluorescence and Western blotting. Cells seeded on coverslips were fixed with 3.7% formaldehyde at different time points after release from cell cycle arrest, dehydrated with cold methanol and acetone, and permeabilized with 0.2% Triton X-100. After successive washes with 0.2% Tween 20, 0.2% Triton X-100 in PBS, and 2 mM $MgCl_2$ in PBS, cells were preincubated with normal goat serum for 1 h, followed by successive incubations with a rabbit polyclonal antibody (SP8) that is directed against NS1 (16) for 2 h and a second anti-rabbit immunoglobulin G conjugated with Oregon Green 488 (Molecular Probes, Eugene, Oreg.) for 1 h. Cells were washed again as described above and stained with DAPI (4′,6′-diamidino-2-phenylindole) for 1 min, rinsed in water, and dehydrated in ethanol. Coverslips with cells were then mounted on slides and observed under a fluorescence microscope (Leica DMIBE). The percentage of NS1-positive cells was calculated by counting the numbers of NS1-positive versus DAPI-stained cells in the same microscopic fields. A minimum of 100 DAPI-stained cells was counted.

For Western blotting, synchronized or unsynchronized cells infected with the H-1 virus were washed with PBS and lysed in RIPA buffer (10 mM Tris-HCl [pH 7.5], 150 mM NaCl, 1 mM EDTA, 1% Nonidet P-40, 0.5% sodium deoxycholate, 0.1% sodium dodecyl sulfate) containing protease inhibitors (Roche Diagnostics). Cell lysates were measured for protein amounts by using a Bradford assay. Equal amounts of cell lysates (30 to 40 μg) were fractionated by sodium dodecyl sulfate-polyacrylamide gel electrophoresis and transferred onto nitrocellulose membranes. Nonspecific binding was blocked by incubating membranes in 5% nonfat milk for 1 h at room temperature. The membrane was then incubated in the same solution with NS1-specific antiserum (SP8) overnight at 4°C, washed with 0.5% Tween 20 in PBS, probed with horseradish peroxidase-conjugated second antibody for 1 h at room temperature, washed again as described above, and, finally, the immunocomplex was revealed by enhanced chemiluminescence analysis (Amersham Pharmacia Biotech). Other antibodies used were directed against human c-Myc (sc-40; Santa Cruz), Id1 (sc-488; Santa Cruz), CEBPβ (sc-150; Santa Cruz), caspase-8 (catalog no. 551242; BD Pharmingen), c-Jun (catalog no. 554083; BD Pharmingen), PARP-1 (C2-10; eBioscience, San Diego, Calif.), and α-tubulin (Sigma).

Sample preparation and hybridization to DNA chips. Total RNA was extracted by using an RNeasy Mini kit (QIAGEN). RNA was assessed for its quality by 1% formaldehyde-denaturing agarose gel electrophoresis and for its quantity by spectrophotometric measurement (Biophotometer; Eppendorf). Two independent experiments were set for array hybridization. In each experiment, total RNAs from two plates (each containing 10^6 cells) were pooled. Total RNA (20 μg) was reverse transcribed into double-strand cDNA with T7 primers (SuperScript Choice System; Life Technologies, Inc.). After phenol-chloroform extraction, cDNA was transcribed into biotinylated RNA targets (RNA transcript labeling kit; Affymetrix), purified (RNeasy Mini kit; QIAGEN) and fragmented according to the manufacturer's instructions.

Hybridization was performed by following the Affymetrix standard protocol. Briefly, the samples were first tested for RNA integrity with test chips (Test3 array; Affymetrix). cRNA samples which passed this test were loaded onto human genome U133A chips (Affymetrix) in duplicate. After hybridization, the chips were stained and washed in a Genechip Fluidics Station 400 (Affymetrix) and scanned by using a Genechip Array scanner (Affymetrix).

TABLE 1. Primers used in quantitative real-time RT-PCR

Gene product	Primer sequence		Length of product (bp)
	Forward	Reverse	
MYC	5′-CTTGTTTCAAATGCATGATCAAATGCAACC	5′-CATAAAAAAGTTCTTTTATGCCCAAAGTCC	122
CEBPD	5′-GGAGCGCAAAGAAGCTACAGCCTGGAC	5′-TTTTTCTTTTTACAAATGTACCTTAGCTGC	153
ARHB	5′-AAAATTTAGTGGGTTTCTTTTCCCTCTCC	5′-TGTTTCATTGTTTGACACTTAATGCACTCG	148
DUSP2	5′-GCTGGCCCTCATTCGGGGTCGG	5′-GCCAAGGGCTTCAACATGGTGGTGGAC	128
DKK1	5′-GAGCTTTGTTTCTTTATGGAACTCCCCTG	5′-CAAGAGGAAAAATAGGCAGTGCAGCACC	141
ID3	5′-CGTCACCCTGCTCCCACCCCACC	5′-TCCAAGGAGACCAGAAGACCAGCTCTGC	125
TGIF	5′-TAAACTTAAAGCTACTGTAGAAACAAAGGG	5′-AGTATGTGGGCATCCTGTTCCACATGGG	205
FOXF2	5′-CAGTGCTAAGCACAAGATTTCAAGAAAGCC	5′-AATAATTCCTTAATAATGTTCTTTGGCACC	120
TIEG	5′-TTAATTTATAGGAGTTTTTTGGGGATGTGG	5′-ATATTTTAAGCAATGTACTTTTGTTTTGCC	150
TNFRSF6B	5′-GCCAGGATGCCCGGGCTGGAG	5′-CCTCATTTCTTCTATTTAAAAAAAAGCCTC	140
UREB1	5′-TGCTGCCCTCGAAGGCATGAATGG	5′-ATAGCCAACAGTAGCATGTGGCGGAGC	159
TFRC	5′-AATTTTAAGTGCTTTGTAATGGGAACTGCC	5′-GTTGGAGGATCACTCAAAGTAAGCGACCAC	160

Data processing. The signal intensities of each array were collected, normalized, and compared by using MAS 5.0 software (Microarray Suite 5.0; Affymetrix) and further analyzed with Data Mining Tool software (Affymetrix). A pair-wise comparison was performed between two sets (infected versus mock-treated cells) of replicate samples. The genes were retained for further analysis if they met the following criteria. (i) For up- or down-regulated genes, detection was considered "present" in at least one of the two virus- or mock-infected samples, respectively, and signal intensity was above 20 when detection is present. The signal intensities of absent detection of below 20 were adjusted to 20. (ii) Among the four possible combinations of comparison, the genes whose changes scored as either an increase or a decrease in at least three of the comparisons were retained. (iii) Among the four combinations of log ratio values (base 2), the genes up-regulated with a low log ratio of signal intensity of greater than 0.1 or down-regulated with a high log ratio of signal intensity of less than 0.1 with at least a 95% confidence interval were retained. The log ratio values were subsequently converted to changes (*n*-fold) in regulation.

Quantitative real-time RT-PCR. Total RNA (10 μg) was reverse transcribed into cDNA by using a LightCycler-FastStart DNA master SYBR Green I kit (Roche Diagnostics). cDNAs were diluted 1:5 or 1:10, and 0.5 μM concentrations of primers (MWG Biotech AG) were used in all reactions. The same volumes of cDNA preparations (2 μl) were taken for each subsequent reaction. Real-time reverse transcription (RT)-PCR was performed in duplicate by using a LightCycler apparatus (Roche Diagnostics). The reactions started with an 8-min incubation at 95°C, followed by 45 cycles of denaturation (15 s at 95°C), annealing (5 s at 62°C), and elongation (10 s at 72°C). An additional 3 s at 82°C was set for fluorescence measurement. The copy numbers of different mRNAs were calculated by using their threshold crossing (Ct) value and a standard curve. UREB1 (upstream regulatory element binding protein 1) mRNA, which shows stability in this system, was used as the internal control. The primer sequences used for the real-time RT-PCR analysis of distinct cellular genes were designed by means of the Oligo 8.40 program (Rusian Kalendar, Institute of Biotechnology, University of Helsinki) and are listed in Table 1. The primers for H-1 transcripts correspond to a region bracketing the end of NS1 and the beginning of VP.

Promoter analysis. The EZ-Retrieve program (73) was used to retrieve the promoter sequences of selected genes and to search for the occurrence of transcription factor binding sites within promoter regions.

RESULTS

Status of synchronized cells after H-1 virus infection: cell cycle distribution, NS1 expression, and cell mortality. In order to select the time points for gene expression profiling and follow up on the corresponding status of cells, we monitored the cell cycle distribution, expression of the viral nonstructural protein NS1, and cell mortality at different time points after virus infection.

Considering the fact that individual cells will start to replicate parvovirus only when entering into S phase, the analysis of cellular disturbance occurring in the course of infection required the use of a highly homogenous population of cells regarding the cell cycle distribution. This homogeneity was achieved by synchronizing QGY-7703 cells prior to infection by using mimosine, a tyrosine analogue functioning as a specific and reversible late-G_1 blocker of the cell cycle (29). Cells were first arrested in the presence of mimosine and then infected 8 h prior to removal of the drug (Fig. 1). Since mimosine is able to arrest replication of parvoviruses (14), this protocol ensures a synchronous onset of H-1 virus replication and gene expression upon release from the drug treatment.

As measured by FACScan analysis, about 60% of the cells from asynchronous QGY-7703 cultures were in G_1 phase (Fig. 2A). After mimosine treatment, a high degree of synchronization was achieved during at least one cell cycle (Fig. 2B). In the presence of the drug, more than 90% of cells were arrested at G_1 phase (Fig. 2B, 0 h). After removal of the drug, uninfected cultures synchronously entered S phase (about 90% of the cells from 6 to 9 h postrelease), reached G_2 phase (more than 60%

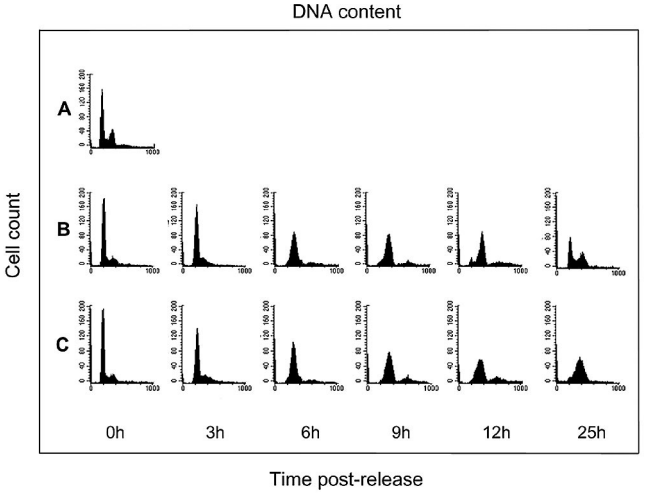

FIG. 2. Cell cycle distribution of mock- or virus-infected synchronized QGY-7703 cultures. Cells harvested at various time points after release from mimosine treatment were fixed with 75% ethanol, stained with DAPI, and subjected to FACScan analysis. (A) Untreated control. (B) Mock-treated cells. (C) H-1 virus-infected cells.

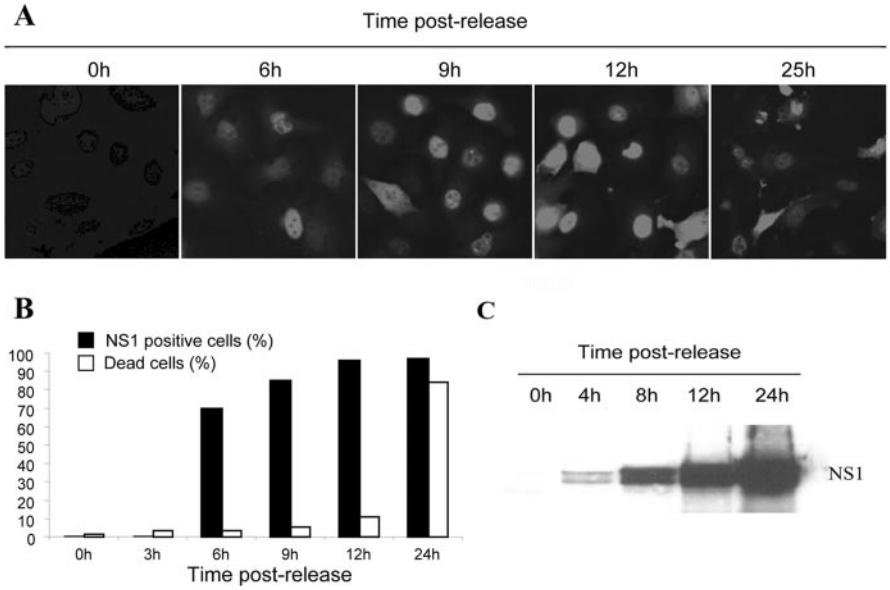

FIG. 3. NS1 expression in synchronized QGY-7703 cells. At different time points after release from mimosine treatment, cells seeded on coverslips were fixed. After incubation with antiserum against the viral protein NS1 (SP8) and secondary antibodies conjugated with Oregon Green 488, preparations were stained with DAPI and observed under a fluorescence microscope. The percentages of NS1-expressing cells were calculated by counting the numbers of NS1-positive versus DAPI-stained cells in the same microscopic fields. Representative pictures are shown for each time point. The percentages of dead cells were calculated by counting the numbers of trypan blue-positive cells versus total cells by using a hemocytometer. (A) Immunofluorescence analysis of NS1 expression. (B) Percentages of NS1-positive and dead cells. (C) Western blotting detection of NS1 proteins. The two bands correspond to phosphorylated and hyperphosphorylated forms of the polypeptide.

of the cells at 12 h), and completed the first cell cycle (all cells at 25 h).

Synchronized cultures infected with wild-type H-1 virus at a MOI of 10 PFU/cell showed a cell cycle distribution similar to that of mock-treated cells up to 12 h postrelease (Fig. 2B versus 2C). Differences in cell cycle distribution between mock-treated and H-1 virus-infected cells became visible at later times. H-1 virus-infected cells became irreversibly arrested in G_2 phase and eventually died, whereas in mock-treated cultures, the cell cycle progressed up to completion and proceeded to the next one.

The expression of the NS1 protein, an indicator of the synthesis and further amplification of viral DNA replicative forms, was monitored in infected cells by immunofluorescence assays. NS1-positive cells were first detected at about 4 h postrelease (~10% of the culture; data not shown) and increased in number with time, reaching 95% of the population at 12 h postrelease (Fig. 3B). A time-dependent enhancement of fluorescence intensity was also observed (Fig. 3A). At 12 h, a few cells started to show cytopathic effect as monitored by both light and immunofluorescence microscopy. At subsequent times, infected cells got swollen and deformed, indicating the progression of viral cytocidal effects. No induction of apoptotic bodies was detected in this system (data not shown).

In parallel, the cell mortality was monitored at each time point by using the trypan blue exclusion method. While less than 10% of the cells were dead during the first 12 h postrelease, this number increased to 83% between 12 h and 24 h, corresponding to the percentage of NS1-positive cells at 24 h (Fig. 3B).

To minimize as much as possible the differences in cell cycle distribution between the cell populations under comparison, i.e., H-1 virus-infected versus buffer (mock)-treated cells, we chose 6 and 12 h postrelease as the time points for gene expression profiling. At these time points, H-1 virus- and mock-treated cultures had similar cell cycle patterns and mortality was low among infected cells, although NS1 expression was high. In other words, virus replication was under way during this period, but the ensuing cell disturbances were still barely visible.

General characteristics of the cellular gene expression profile after virus infection. mRNAs isolated at 6 and 12 h postrelease from two independent experiments, each performed in duplicate, were converted into cRNAs and loaded first on Test3 chips and then on U133A chips. The integrity of mRNAs and cRNAs was confirmed by using formaldehyde-denaturing agarose gels and test chips, respectively (data not shown). After hybridization, signal intensities were measured and analyzed by using MAS 5.0 software. For samples harvested at 6 h postrelease, the correlation coefficient between separate experiments for both buffer (mock)-treated (mock 1 versus mock 2) and virus-infected (virus 1 versus virus 2) samples was 0.994. For samples harvested at 12 h, these coefficients were 0.975 (mock 1 versus mock 2) and 0.980 (virus 1 versus virus 2), respectively. This result indicates that the RNA samples used were of high homogeneity and that the experiments were reproducible.

About 50% of the genes on the chips (~10,800 genes) were detected in this system. Using the criteria described in Materials and Methods, with a ±2.5-fold change as the threshold, we identified 105 genes that were differentially expressed at the mRNA level between virus-infected and mock-treated cells at

TABLE 2. Number of regulated genes at different changes (*n*-fold) in expression[a]

Fold change	No. of regulated genes at indicated time postrelease			
	6 h		12 h	
	Up	Down	Up	Down (%)[b]
1.3	20	26	24	471 (95)
2.0	1	1	12	222 (95)
2.5	1	0	7	98 (93)

[a] Genes were selected according to the criteria described in Materials and Methods. Up, up-regulated; Down, down-regulated.
[b] Percentages of down-regulated genes among the regulated genes at 12 h are shown in parentheses.

12 h postrelease, which accounts for only 1% of the detected genes. The majority (93%) of these genes were underexpressed in infected cells (Table 2). At 6 h postrelease, the expression of only one of these genes was found to be already affected by virus infection according to the criteria above, although more than 60% of cells were NS1 positive at this time point. In this experiment, we regard expression changes of more than 2.5-fold as significant. However, if the threshold was lowered to 1.3-fold, 11 distinct genes whose mRNAs were modulated at 12 h already showed expression changes at 6 h postrelease (Table 3). These data indicate that the virus-induced alterations of cellular gene expression start as early as 6 h postrelease but that they require further progression of the viral cycle to become prominent. The sensitivity of the microarray methodology as an indicator of virus-induced perturbations is also worth noting. This approach allowed distinct molecular changes to be detected in infected cells at a time (12 h postrelease) when no or little cytopathic effects and cell cycle alterations were visible (Fig. 2B and C). Among the genes modulated at 12 h, 19 candidates encode hypothetical proteins or proteins of unknown function. The other 86 candidates are known and comprise a great majority (82%) of genes whose products cluster mainly into the following functional groups: transcription regulation, signal transduction, growth and apoptosis, and immune and stress responses (Table 3). It should be stated that many of these genes are multifunctional and are assigned to more than one functional class. In each class, the number of down-regulated genes was much higher than that of up-regulated ones, reflecting a general trend in the cellular transcription dysregulation induced by parvovirus H-1.

Confirmation of microarray data with quantitative real time RT-PCR. Eleven genes were selected on the basis of microarray data for confirmation by quantitative PCR. Among the genes, nine showed >2.5-fold changes in array experiments, eight of them being down-regulated (*MYC*, *ARHB*, *DKK1*, *CEBPD*, *DUSP2*, *ID3*, *TGIF*, and *FOXF2*) and one of them being up-regulated (*TNFRSF6B*). The *GAPDH* and *TFRC* (transferrin receptor) genes were included but did not show significant changes in mRNA levels. Real-time quantitative RT-PCR was performed with RNA samples from the same pool used for microarray experiments, as well as with samples from an independent infection experiment using synchronized cells. Both the type of gene expression modulation (up or down) and the relative mRNA abundance of all the candidates were in agreement with the microarray data, with only some variations (*n*-fold) in the values (Table 4). These data therefore give credence to the validity of the microarray results.

Time-course analysis of virus-induced changes in the levels of specific mRNAs. In array experiments, gene expression profiles were determined at two time points after virus infection. In order to monitor the gene expression changes over time after virus infection, the mRNA levels of seven genes whose expression was found to be modulated in array experiments were monitored. RNA was isolated from virus- or mock-infected cells at four time points (6, 9, 12, and 18 h postrelease) and quantified by real-time quantitative RT-PCR (qRT-PCR). Data were normalized to upstream regulatory element binding protein 1 (UREB1) transcripts whose abundance showed stability during the time period under investigation.

As shown in Fig. 4A to G, mRNAs from mock-treated samples kept relatively stable over time, although some variations were observed, possibly due to the cell cycle progression through S to G_2/M and early G_1 phases (corresponding to 6 to 18 h postrelease). In contrast, the mRNAs from virus-infected cells underwent clear-cut changes in agreement with the array data: the six genes (*MYC*, *ARHB*, *DKK1*, *DUSP2*, *ID3*, and *CEBPD*) that were down-regulated according to the latter method showed a progressive decrease of mRNA levels with time after infection, while the up-regulated gene (*TNFRSF6B*) showed an increase in mRNA during this interval. The difference between the mRNA levels of mock-treated and virus-infected samples increased over time for all of the genes tested. During the same period, virus transcripts (Fig. 4H) and NS1 proteins (Fig. 3C) kept accumulating in a continuous fashion. A positive correlation could thus be drawn between the extent of cellular gene expression changes and the accumulation of viral products. Although it was not feasible to check mRNA variations with qRT-PCR for all of the candidate genes identified in array experiments, it is reasonable to assume that the virus-induced perturbation of the whole cell gene expression profile parallels the production of viral cytotoxic proteins.

Western blot analysis of candidate proteins. Protein contents do not necessarily reflect the levels of corresponding mRNAs due to the occurrence of various posttranscriptional regulations. To determine whether the virus-induced RNA changes detected by means of array and/or qRT-PCR affected the abundance of the corresponding proteins, several candidates were subjected to Western blotting. Unsynchronized cultures were infected with the H-1 virus at a MOI of 10 PFU/cell and harvested at 0, 11, 24, 32, and 48 h postinfection. The extent of cell mortality observed at 48 h in these cultures was similar to that detected at the 24-h time point under above synchronized conditions (data not shown).

Four of the candidates tested were transcription factors. c-Myc and c-Jun are related to cell proliferation, growth, and, under certain conditions, apoptosis (37, 49). Id1 is a negative regulator of cell differentiation but also a strong inducer of apoptosis when overexpressed (43). CEBPβ is involved in immune and inflammatory responses (38). c-Myc, c-Jun, and Id1 showed a decrease over time after infection (Fig. 5), indicating that the virus-induced alteration of the steady-state amounts of corresponding transcripts was reflected at the protein level. In contrast, the CEBPβ protein underwent a slight decrease over time, suggesting that some posttranscription regulation com-

TABLE 3. Genes differentially expressed in H-1 virus-infected cells at 12 h postrelease[a]

Function and gene product	Description	Fold change at:		Accession no.
		6 h	12 h	
Transcription and nuclear processes				
MYC	v-*myc* myelocytomatosis viral oncogene homolog (avian)		−5.2	NM_002467
HR	Hairless		−5.0	AF039196
FOS	v-*fos* FBJ murine osteosarcoma viral oncogene homolog		−4.7	BC004490
HEY1	Hairy/enhancer-of-split related with YRPW motif 1		−4.5	NM_012258
CEBPB	CCAAT/enhancer binding protein (C/EBP), beta		−4.2	AL564683
SOX4	SRY (sex-determining region Y)-box 4		−4.0	NM_003107
TCF8	Transcription factor 8 (represses interleukin 2 expression)		−4.0	NM_030751
KLF4	Kruppel-like factor 4 (gut)		−3.9	BF514079
HHEX	Hematopoietically expressed homeobox		−3.7	Z21533
TIEG	TGFB-inducible early growth response		−3.7	NM_005655
IKBA	Nuclear factor of kappa light polypeptide gene enhancer in B-cell inhibitor, alpha		−3.6	NM_020529
TBX3	T-box 3		−3.6	NM_016569
ELF3	E74-like factor 3		−3.6	U73844
ID3	Inhibitor of DNA binding 3		−3.6	NM_002167
KLF13	Kruppel-like factor 13		−3.5	NM_015995
ZPF36LI	Zinc finger protein 36		−3.5	BE620915
ID1	Inhibitor of DNA binding 1	−1.3	−3.4	D13889
CITED2	Cbp/p300-interacting transactivator		−3.4	NM_006079
GIOT3	GIOT-3 for gonadotropin inducible transcription repressor-3		−3.4	NM_016265
COPEB	Core promoter element binding protein		−3.3	BE675435
LOC58486	Transposon-derived Buster1 transposase-like protein		−3.3	NM_021211
TGIF	TGFB-induced factor (TALE family homeobox)		−3.3	NM_003244
CEBPD	CCAAT/enhancer binding protein (C/EBP), delta		−3.2	M83667
TSC22	Transforming growth factor beta-stimulated protein TSC-22		−3.2	AK027071
ETS2	v-*ets* erythroblastosis virus E26 oncogene homolog 2 (avian)		−3.1	AL575509
MEOX1	Mesenchyme homeobox 1		−3.1	NM_004527
DLX2	Distal-less homeobox 2		−3.0	NM_004405
FOXF2	Forkhead box F2		−3.0	NM_001452
BHLHB2	Basic helix-loop-helix domain containing, class B, 2		−2.9	NM_003670
EN1	Engrailed homolog 1		−2.8	NM_001426
NR3C1	Nuclear receptor subfamily 3, group C, member 1 (glucocorticoid receptor)		−2.7	X03348
JUNB	JunB proto-oncogene		−2.7	NM_002229
MADH7	MAD, mothers against decapentaplegic homolog 7 (*Drosophila*)		−2.7	NM_005904
HOXA10	Homeobox A10		−2.7	AI375919
TFAP2A	Transcription factor AP-2 alpha		−2.6	NM_003220
ZF	HCF-binding transcription factor Zhangfei		−2.5	NM_021212
NFIL3	Nuclear factor, interleukin 3 regulated		−2.5	NM_005384
POGK	Pogo transposable element with KRAB domain		−2.5	NM_017542
ZCCHC2	Zinc finger, CCHC domain containing 2		−2.5	BE676543
JUN	v-*jun* sarcoma virus 17 oncogene homolog (avian)	−1.5	−2.5	BC002646
Signal transduction				
ARHB	Ras homolog gene family, member B		−5.5	AI263909
CXCR4	Chemokine (C-X-C motif) receptor 4	−1.4	−5.0	AF348491
DUSP2	Dual-specificity phosphatase 2		−4.3	NM_004418
VAV3	Vav 3 oncogene		−4.1	NM_006113
ADAMTS1	A disintegrin-like and metalloprotease with thrombospondin type 1 motif, 1	−1.5	−4.0	AK023795
DKK1	Dickkopf homolog 1 (*Xenopus laevis*)	−1.5	−4.0	NM_012242
ADM	Adrenomedullin		−4.0	NM_001124
SGK	Serum/glucocorticoid-regulated kinase	−1.4	−3.9	NM_005627
DUSP1	Dual-specificity phosphatase 1		−3.8	NM_004417
ARL4	ADP-ribosylation factor-like 4	−1.4	−3.7	NM_005738
TIEG	TGFB-inducible early growth response		−3.7	NM_005655
ZPF36L1	Zinc finger protein 36, C3H type-like 1		−3.5	BE620915
FEM1B	Fem-1 homolog b (*Caenorhabditis elegans*)		−3.5	NM_015322
CDC42EP3	CDC42 effector protein (Rho GTPase binding) 3		−3.5	AI754416
PTGER4	Prostaglandin E receptor 4 (subtype EP4)		−3.3	AA897516
EFNA1	Ephrin-A1		−3.2	NM_004428
SNK	Serum-inducible kinase		−3.2	NM_006622
MFHAS1	Malignant fibrous histiocytoma amplified sequence 1		−3.2	BF739959
RANBP6	RAN binding protein 6		−3.1	AI123233
NMA	Putative transmembrane protein		−3.0	NM_012342
SOCS4	Suppressor of cytokine signaling 4		−2.9	NM_016387
DUSP7	Dual specificity phosphatase 7		−2.9	AI655015
BHLHB2	Basic helix-loop-helix domain containing, class B, 2		−2.9	NM_003670
C8FW	Phosphoprotein regulated by mitogenic pathways		−2.8	NM_025195
FGF2	Fibroblast growth factor 2 (basic)		−2.7	M27968
MADH7	MAD, mothers against decapentaplegic homolog 7 (*Drosophila*)		−2.7	NM_005904
TXNIP	Thioredoxin-interacting protein		−2.7	NM_006472
SOCS5	Suppressor of cytokine signaling 5		−2.7	NM_014011
PNRC2	Proline-rich nuclear receptor coactivator 2		−2.7	NM_017761
VEGF	Vascular endothelial growth factor		−2.6	AF022375

Continued on following page

TABLE 3—*Continued*

Function and gene product	Description	Fold change at:		Accession no.
		6 h	12 h	
TNFSF9	Tumor necrosis factor (ligand) superfamily, member 9		−2.6	NM_003811
WNT5A	Wingless-type MMTV integration site family		−2.5	NM_003392
Growth and apoptosis				
TNFRSF6B	Tumor necrosis factor receptor superfamily, member 6b, decoy	1.9	3.4	NM_003823
GAS1	Growth arrest-specific 1		−7.5	AW611727
RTP801	HIF-1-responsive RTP801	−1.5	−5.8	NM_019058
MYC	v-*myc* myelocytomatosis viral oncogene homolog (avian)		−5.2	NM_002467
CXCR4	Chemokine (C-X-C motif) receptor 4	−1.4	−5.0	AF348491
FOS	v-*fos* FBJ murine osteosarcoma viral oncogene homolog		−4.7	BC004490
DKK1	Dickkopf homolog 1 (*X. laevis*)	−1.5	−4.0	NM_012242
TIEG	TGFB-inducible early growth response		−3.7	NM_005655
JKBA	Nuclear factor of kappa light polypeptide gene enhancer in B-cells inhibitor, alpha		−3.6	NM_020529
ID3	Inhibitor of DNA binding 3		−3.6	NM_002167
ZPF36L1	Zinc finger protein 36, C3H type-like 1		−3.5	BE620915
FEM1B	Fem-1 homolog b (*C. elegans*)		−3.5	NM_015322
ID1	Inhibitor of DNA binding 1	−1.3	−3.4	D13889
EFNA1	Ephrin-A1		−3.2	NM_004428
C8FW	Phosphoprotein regulated by mitogenic pathways		−2.8	NM_025195
BTG1	B-cell translocation gene 1		−2.8	NM_001731
FGF2	Fibroblast growth factor 2 (basic)		−2.7	M27968
JUNB	Jun B proto-oncogene		−2.7	NM_002229
SOCS5	Suppressor of cytokine signaling 5		−2.7	NM_014011
TNFSF9	Tumor necrosis factor (ligand) superfamily, member 9		−2.6	NM_003811
JUN	v-*jun* sarcoma virus 17 oncogene homolog (avian)	−1.5	−2.5	BC002646
Immune and stress response				
TNFRSF6B	Tumor necrosis factor receptor superfamily, member 6b, decoy	1.9	3.4	NM_003823
KNG	Kininogen		3.1	NM_000893
CXCR4	Chemokine (C-X-C motif) receptor 4	−1.4	−5	AF348491
FOS	v-*fos* FBJ murine osteosarcoma viral oncogene homolog		−4.7	BC004490
DUSP2	Dual-specificity phosphatase 2		−4.3	NM_004418
CEBPB	CCAAT/enhancer binding protein (C/EBP), beta		−4.2	AL564683
TCF8	Transcription factor 8 (represses interleukin 2 expression)		−4.0	NM_030751
ADAMTS1	A disintegrin-like and metalloprotease with thrombospondin type 1 motif, 1	−1.5	−4.0	AK023795
ADM	Adrenomedullin		−4.0	NM_001124
DUSP1	Dual specificity phosphatase 1		−3.8	NM_004417
HHEX	Hematopoietically expressed homeobox		−3.7	Z21533
PTGER4	Prostaglandin E receptor 4 (subtype EP4)		−3.3	AA897516
EFNA1	Ephrin-A1		−3.2	NM_004428
CEBPD	CCAAT/enhancer binding protein (C/EBP), delta		−3.2	M83667
NR3C1	Nuclear receptor subfamily 3, group C, member 1 (glucocorticoid receptor)		−2.7	X03348
MADH7	MAD, mothers against decapentaplegic homolog 7 (*Drosophila*)		−2.7	NM_005904
NFIL3	Nuclear factor, interleukin 3 regulated		−2.5	NM_005384
Cell cycle				
GAS1	Growth arrest-specific 1		−7.5	AW611727
MYC	v-*myc* myelocytomatosis viral oncogene homolog (avian)		−5.2	NM_002467
MFHAS1	Malignant fibrous histiocytoma amplified sequence 1		−3.2	BF739959
BTG1	B-cell translocation gene 1		−2.8	NM_001731
COIL	Coilin		−2.7	NM_004645
DNA2L	DNA2 DNA replication helicase 2-like (yeast)		−2.6	D42046
BCAR3	Breast cancer anti-estrogen resistance 3		−2.5	NM_003567
Transport and membrane				
KCC2	Solute carrier family 12	3.6	3.3	AF208159
SGK	Serum/glucocorticoid-regulated kinase	−1.4	−3.9	NM_005627
ZNT1	Solute carrier family 30 (zinc transporter), member 1		−3.1	AI972416
SLC11A2	Solute carrier family 11 (proton-coupled divalent metal ion transporters), member 2		−2.7	AF046997
BLCAP	Bladder cancer-associated protein		−2.5	NM_006698
RNA and protein processing				
RBAF600	Retinoblastoma-associated factor 600	1.5	2.9	AB007931
DDX28	DEAD/H (Asp-Glu-Ala-Asp/His) box polypeptide 28		−5.5	NM_018380
FBXO5	F-box-only protein 5		−4.6	NM_012177
SCA1	Spinocerebellar ataxia 1		−3.8	NM_000332
GEMIN4	Gem (nuclear organelle)-associated protein 4		−2.6	NM_015487
Other				
TTN	Titin		4.0	NM_003319
FLJ23058	Hypothetical protein FLJ23058		2.8	NM_024696

Continued on following page

TABLE 3—*Continued*

Function and gene product	Description	Fold change at:		Accession no.
		6 h	12 h	
ZG16	Zymogen granule protein 16		2.5	AI732905
C8orf4	Chromosome 8 open reading frame 4		−4.7	NM_020130
C6orf37	Chromosome 6 open reading frame 37		−4.6	AW246673
PPP1R3C	Protein phosphatase 1, regulatory (inhibitor) subunit 3C		−3.7	N26005
PPP1R3D	Protein phosphatase 1, regulatory subunit 3D		−3.1	AL109928
FLJ10374	Hypothetical protein FLJ10374		−2.9	NM_018074
FLJ21870	Hypothetical protein FLJ21870		−2.8	NM_023016
AMIGO2	Amphoterin induced gene 2		−2.8	AC004010
NPD014	Hypothetical protein dJ465N24,2,1		−2.8	AF247168
KIAA0469	KIAA0469 gene product		−2.7	NM_014851
OSR2	Odd-skipped-related 2A protein		−2.7	AI811298
LOC90355	Hypothetical gene supported by AF038182		−2.7	AL565741
MAT2A	Methionine adenosyltransferase II, alpha		−2.5	BC001686
FLJ20508	Hypothetical protein FLJ20508		−2.5	NM_017850
METTL2	Methyltransferase like 2		−2.5	NM_018396
FLJ20257	Hypothetical protein FLJ20257		−2.5	NM_019606
FLJ12178	Hypothetical protein		−2.5	AI742305
MIS12	Homolog of yeast Mis12		−2.5	BC000229

[a] Positive and negative changes represent overexpression and underexpression (*n*-fold) in virus-infected versus mock-treated cells, respectively. Genes showing changes (*n*-fold) lower than −2.5 or higher than +2.5 at 12 h postrelease are listed. Changes at 6 h are listed only for the genes with those above 2.5-fold at 12 h. Some genes are grouped into more than one class due to their multiple functions.

pensated for the observed drops in the levels of corresponding mRNAs.

It was reported that treatment with TRAIL or etoposide can induce apoptosis in QGY-7703 cells, accompanied by activation of caspases and PARP (39). It is also documented that parvovirus H-1 causes apoptosis in several cell lines, including hepatoma cells (40). However, we failed to detect signs of apoptosis, such as apoptotic bodies, DNA ladders (data not shown), and sub-G_1 peaks (Fig. 2C), in QGY-7703 cells infected with the H-1 virus. The above-mentioned *MYC*, *JUN*, and *ID1* proapoptotic genes were found to be down-regulated in virus-infected QGY-7703 cells, and a gene encoding death domain inhibitor (*TNFRSR6B*) was up-regulated. This was also the case for other genes whose products contribute to apoptosis (see Table 3). Fas-associated death domain protein (FADD), an essential component of the death receptor apoptotic pathway, was down-regulated 2.2-fold. This finding led us to speculate that the ability of the H-1 virus to trigger apoptosis cascade in this cell line is impaired. This hypothesis was tested by analyzing distinct components of this cascade.

TABLE 4. Confirmation of microarray data by quantitative real-time RT-PCR[a]

Gene product	Fold change determined by:		
	Array	RT-PCR	
		A	B
ARHB	−5.5	−5.2	−3.8
MYC	−5.2	−7.1	−5.4
DUSP2	−4.3	−4.1	−3.1
ID3	−3.6	−4.2	−3.5
DKK1	−4.0	−2.1	−3.7
CEBPD	−3.2	−3.4	−3.5
TGIF	−3.3	−3.2	–
FOXF2	−3.0	−2.7	–
TNFRSF6B	3.4	–	4.3
TFRC	NC	1.1	1.3
GAPDH	NC	–	−1.1

[a] A, values were obtained by using the same RNA as for the array experiment; B, values were obtained by using RNA from an independent experiment; average values from two PCRs are given. NC, no change; –, not available.

Apoptosis is initiated through the activation of caspase-8 or caspase-9, leading to the subsequent activation of downstream effectors caspase-3 and caspase-7, which cleave specific substrates. One of these substrates, PARP-1, is a multifunctional enzyme that catalyzes the formation of poly(ADP-ribose) polymers on acceptor proteins involved in the maintenance of chromatin structure and DNA repair and is considered to be an indication of the activation of the apoptotic cascade (61). No virus-induced changes in the abundance of caspase-related mRNAs were detected in array experiments. To confirm that the H-1 virus was indeed unable to activate these proteins, the cleavages of procaspase-8 and PARP-1 were measured in the course of time after infection. Antibodies recognizing both proproteins and their cleaved fragments were used to this end. As shown in Fig. 5, H-1 virus infection not only resulted in a decrease of the procaspase-8 steady-state level, but also failed to induce the cleavage of residual proenzymes into characteristic 40-, 36-, and 23-kDa fragments. Similarly, no 85-kDa cleavage product of PARP-1 in infected cells could be detected, indicating that caspase-3 and caspase-7 were not activated in this system. Altogether, these observations lead us to conclude that (i) several intermediates of apoptotic cascades are down-regulated as a result of H-1 virus infection of QGY-7703 cells, (ii) this dysregulation can take place at both transcriptional and posttranscription levels, and (iii) these changes correlated with the inability of the H-1 virus to induce apoptosis in these cells.

Promoter analysis of modulated genes. The differences observed in the levels of specific mRNAs between mock- and virus-infected cells are likely to be due to a large extent to transcriptional regulation, although some effects of the H-1 virus in mRNA stability cannot be ruled out. The parvoviral NS1 protein is a site-specific transregulator which proved able to repress or activate a few homologous and heterologous promoters (18, 54, 67); therefore, the occurrence of NS1 binding sites $(ACCA)_{2–3}$ in the promoters (500 bp in length) of 7

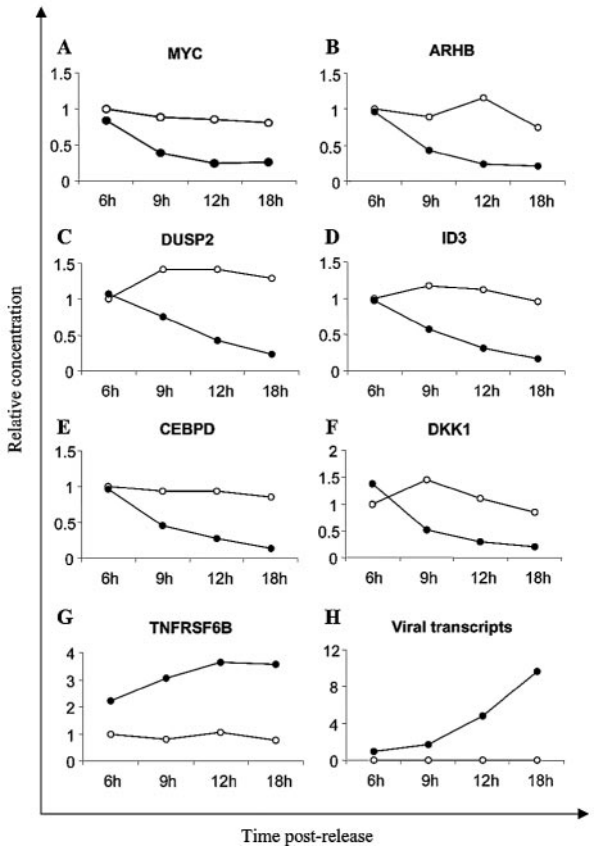

FIG. 4. Variations of selected mRNA levels with time. The relative amounts of transcripts from cellular (A to G) and viral H-1 (H) genes were measured. The cellular genes were representative of candidates whose expression was modulated in array experiments. Total RNA isolated from mock-treated or virus-infected synchronized cells at 6, 9, 12, and 18 h postrelease from mimosine treatment was reverse transcribed into cDNA and quantified by real-time RT-PCR. The relative mRNA concentrations were calculated according to the respective cycle numbers with reference to standard curves and normalized to UREB1 transcripts. For each gene, the mRNA contents are expressed relative to the concentration at 6 h in mock-treated cells (set as 1). The concentrations of this gene at other time points are values relative to 1. The NS1 mRNA concentrations are given relative to the 6 h value in virus-infected cells. Filled circles, virus infected; open circles, mock treated.

up-regulated and 98 down-regulated genes was tested in order to determine whether the H-1 virus induced alteration of the overall cellular gene expression profile may involve the binding of NS1 to the control region of individual target genes. This sequence, which is present at multiple positions throughout the genome of MVM and H-1 viruses, was present in only one of the cellular promoters tested (PPP1R3C [see Table 3]). Therefore, direct binding of NS1 to the $(ACCA)_{2-3}$ motif does not appear to participate in the transcriptional modulation of most cellular target genes. The occurrence of binding sites of other cellular transcription factors, including SP1 and TBP, which were reported to interact with NS1, was also investigated, but no significant difference between the up-regulated and down-regulated genes or between regulated and unregulated control genes was shown.

DISCUSSION

Gene expression profiling reveals trends in H-1 virus–QGY-7703 cell interactions. By means of microarray and quantitative real-time RT-PCR analyses, we identified distinct genes in the hepatoma cell line QGY-7703, whose mRNA steady-state levels were affected as a result of infection with parvovirus H-1. At least part of these changes were unlikely to have been due to cell cycle perturbation, since cells were synchronized and analyzed at early time points after infection, when neither changes in cell cycle distribution nor cytopathic effects could be detected. We reasoned that these conditions enhance the probability that the observed changes in transcript levels are direct consequences of virus infection rather than secondary effects accompanying cell degeneration. As shown in Table 3, four distinct major functional classes of genes are modulated by parvovirus infection.

(i) Transcription and nuclear processes. The largest class deals with transcription regulation and includes genes encoding 40 transcription factors involved in several aspects of cell physiology. Noticeably, several oncogenes that play well-established roles in cell growth and proliferation, such as *MYC*, *ETS2*, and those encoding components of the AP-1 transcription complex (*JUN*, *FOS*, and *JUNB*), were down-regulated upon H-1 virus infection. Two genes (*ID1* and *ID3*) encoding

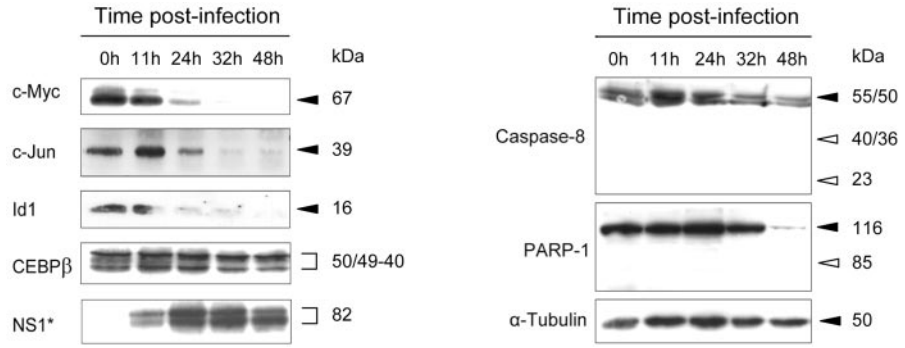

FIG. 5. Western blot analysis of distinct proteins in virus-infected QGY-7703 cells. Cell lysates from asynchronous cultures harvested at various times postinfection were processed for Western blotting by using primary antibodies specific for the indicated proteins and horseradish peroxidase-conjugated secondary antibodies. Blots were revealed through enhanced chemiluminescence. α-tubulin was used as the loading control. Filled arrowheads, measured positions of observed proteins; open arrowheads, expected positions of protein cleavage products; ∗, for NS1, the two bands correspond to phosphorylated and hyperphosphorylated forms of the polypeptide.

the dominant negative helix-loop-helix proteins, which function as negative regulators of differentiation, were also down-modulated at the mRNA level. Moreover, c-Myc, c-Jun, and Id1 were reported to repress thrombospondin-1 (TSP-1), an extracellular matrix glycoprotein and a key inhibitor of neovascularization and tumorigenesis (68). Thus, the repression of these genes may constitute one of the important aspects of this system by which parvoviruses achieve their oncosuppressive activity.

(ii) Signal transduction. The H-1 virus also induced changes in the expression of genes connected to various signaling pathways. ADAMTS1 mediates integrin-mediated signaling, while ARHB belongs to the family of Rho small monomeric GTPases. Interestingly, many of the products of these genes, e.g., the dual specificity phosphatases DUSP1, DUSP2, DUSP7, and the serum/glucocorticoid-regulated kinase SGK play important roles in the cell responses to stresses. In particular, H-1 virus infection results in the repression of several genes that are regulated by HIF-1, a critical intermediate in the response of tumor cells to oxygen depletion (23). Vascular-endothelial growth factor (VEGF) and CXCR4 are up-regulated under hypoxic conditions and promote angiogenesis (34) and metastasis, respectively (63). RTP801 is also activated through HIF-1 and protects cells from hypoxia and H_2O_2-triggered apoptosis via a dramatic reduction in the generation of reactive oxygen species (59). ADM is considered to be a proangiogenic factor (46). Therefore, a number of components of the HIF-1 pathway appear to be a target for parvovirus H-1. Assuming that the proangiogenic/metastatic properties of these genes apply to the present hepatoma system, the data lead us to speculate that suppression of the HIF pathway may contribute to the inhibition of the metastatic and angiogenic properties of tumor cells that would escape the killing effect of the H-1 virus in vivo.

(iii) Growth and apoptosis. Apoptosis is regarded as an innate cellular response to limit virus propagation. As a consequence, a number of viruses have developed strategies to block or delay the death response in host cells by targeting various cellular proteins implicated in the control of apoptosis (17, 20). In the present system, an inhibitor of the Fas death receptor pathway, TNFRSF6B (also designated DcR3), is up-regulated at the mRNA level in H-1 virus-infected cells. Interestingly, overexpression of this protein is employed by several tumors to escape the FasL-dependent toxic activity of immune cells (51). Whether the H-1 virus-mediated activation of TNFRSF6B expression interferes with the apoptotic death of the host cell remains to be experimentally tested. It should be stated that H-1 virus infection also results in the down-regulation of several proapoptotic or apoptosis-related genes, such as *MYC*, *JUN*, *ID1*, *ID3*, *CXCR4*, and *RTP801*, in QGY-7703 cells. Furthermore, the levels of p53 mRNA and protein are very low in this cell line compared with those of some other hepatoma cells (21). Altogether, these data may be correlated with the fact that QGY-7703 cells are killed by the H-1 virus through a nonapoptotic process. It remains to be determined whether this condition is favorable to the completion of a productive H-1 virus infection before cell death takes place. Indeed, QGY-7703 cells have a high capacity for parvovirus H-1 production, whereas infected human leukemia U937 cells, which are similarly sensitive but die from apoptosis, fail to release progeny virions (52). It would be interesting in this regard to compare the H-1 virus bursts produced by QGY-7703 cells and other hepatoma cell lines (Hep3B, Huh-7) which can be distinguished from the former cells by their susceptibility to H-1 virus-induced apoptosis (40).

(iv) Immune and stress response. Additional interesting information provided by the present study is based on the fact that in this system parvovirus H-1 fails to modulate the expression of genes which are usually found to be induced by other viruses as part of a natural response to stresses or pathogens, such as interferons and cytokines. This finding is consistent with a previous report showing that parvoviruses are inefficient in inducing IFN-β, TNF-α, and IL-6 (57) and the observation that parvovirus-infected mice develop a pronounced humoral immune response, whereas the antiviral cellular immune response is low (30). Furthermore, several genes that mediate the stress and immune response (e.g., *CEBPB*, *CEBPD*, *DUSP1*, *VEGF*, *JUN*, and *FOS*) are down-regulated. Altogether, these data speak for the poor ability of parvoviruses to trigger immune and inflammatory signals, a property that is of great interest regarding the safety of parvovirus-based treatments and distinguishes these viruses from many other viral vectors. It should be stated, however, that parvoviruses may still have specific immunomodulating effects, as suggested by a recent paper showing that the H-1 virus induces tumor cells to release the heat shock protein HSP72 (41).

Besides these general trends, some individual genes that are up-modulated by parvovirus H-1 may have a positive impact on virus infection. Such a candidate is the KCl cotransporter KCC2, which plays an important role in ionic and osmotic homeostasis (62), and whose gene is the first to be induced by a factor greater than 2.5 during the course of infection. Further investigations are required to assess the relevance of these genes to the parvoviral life cycle.

Myc is both a positive determinant and a target of parvovirus infection. One of the H-1 virus-sensitive cellular gene products identified in the present study, MYC, plays a key role in the regulation of cell cycle and death and is activated in response to mitogenic factors while being repressed by antiproliferation signals (49). In addition, c-Myc cooperates with other oncoproteins in malignant transformation (49). Brief inactivation of MYC was recently found to cause the irreversible loss of the neoplastic phenotype in osteogenic sarcoma cells (24). It may be expected from the tight dependence of parvoviruses in cell proliferation that MYC contributes in a positive fashion to the permissiveness of host cells to infection with these agents. Accordingly, previous work showed that v-*myc* expression results in the sensitization of transformed rat cells to MVMp-induced cell killing (42, 56). Paradoxically, MYC also appears from the present study to be a target for down-regulation in the course of H-1 infection. Indeed, the abundance of both MYC transcripts and proteins became markedly reduced in response to hepatoma cell infection with H-1. Likewise, we previously found that MYC, which is over expressed in the human promonocytic leukemic cell line U937, is rapidly down-regulated upon infection with both wild-type H-1 virus and a recombinant H-1 derivative (52). Since the latter retained the NS genes but lacked the capsid genes, NS1 was assumed to be responsible for the down-regulation of MYC expression in infected cells. Furthermore, U937 variants

selected for their resistance to H-1 virus infection showed a striking reduction of both their constitutive MYC levels and their tumorigenic phenotypes (35). Altogether, these data indicate that the Myc oncoprotein is not only a determinant but also a target of parvovirus infection and may in this respect play a significant role in the antineoplastic activity of these agents. Additional work is required to assess the impact of the inhibition of MYC expression during progression of the parvovirus life cycle on H-1 virus replication and/or cytotoxic and static effects.

Possible mechanisms of cellular transcription dysregulation by parvoviruses. The cellular gene expression dysregulation presented here is the consequence of wild-type H-1 virus infection, since the virus stock used here was devoid of cellular protein contamination as determined by silver staining and Western blotting (data not shown). The viral effectors of these changes may be assigned to incoming capsids and/or viral proteins that are produced at the rather early infection times studied. The possibility of input capsids altering the patterns of cellular transcripts can be exemplified by a recent work showing that most of the changes in cellular gene expression elicited by full AAV virions can also be induced by empty particles (64). This response required, however, much higher multiplicities of infection than the one used in the present study (MOI, 10). In addition, more than 90% of the virus stock used in the present study consisted of full particles as determined by electron microscopy (data not shown). Yet this finding does not rule out the possibility that the capsids alone, either full or empty, may contribute to some changes in the cellular expression profiles described above. However, the NS polypeptides are likely candidates for disturbers of cellular gene expression. The major nonstructural protein NS1 is of special relevance in this regard, since it is essential for parvovirus cytotoxicity and is endowed with the capacity for transregulating both homologous and heterologous promoters (6, 18, 31, 54, 67). Although it remains to be demonstrated, the role of NS1 in the observed changes in cellular gene expression would be consistent with their time-dependent amplification concomitantly with the accumulation of NS1 proteins. Furthermore, the above-mentioned down-regulation of MYC in H-1 virus-infected human leukemic cells could be achieved by using vectors which lost the ability to code for viral proteins with the exception of NS1 (52). The following discussion will therefore be focused on NS1, although the impact of other parvoviral products cannot be ruled out.

The observed modulation of specific mRNA levels is likely to result, at least in part, from the regulation of the transcription of corresponding cellular genes, although virus-induced destabilization of target mRNAs cannot be excluded. Parvoviruses may modulate transcription through different, nonexclusive routes. One way would involve the direct binding of NS1 and/or its associated cofactors to responsive promoters. NS1 itself is a transcription factor that is endowed with a site-specific DNA-binding capacity (10), but the direct relationship of the DNA-binding property of NS1 and its transregulating ability has not been established. However, the NS1 recognition sequence $(ACCA)_{2\text{-}3}$ was found to be absent from most of the cellular promoters regulated by H-1 virus, arguing against the possibility of NS1 targeting these promoters through direct binding to its cognate motif. On the other hand, NS1 was reported to interact in vitro with ubiquitous cellular transcription factors, such as SP1, TBP, and TFIIA, which may convey NS1 to their respective binding motifs within cellular promoters in the form of a multiprotein complex (36). It should be stated, however, that this possibility could not be substantiated by a search for differences in the occurrence of such motifs between the promoters of NS1-responsive and nonresponsive or poorly responsive genes (data not shown).

Alternatively, NS1 may act indirectly, irrespective of its transregulating function, by modifying components of the transcription machinery that are shared by target promoters. Such a strategy is employed by several viral nonstructural proteins to modulate and, especially, to repress cellular gene expression. For instance, the adenovirus E1A product represses p300-dependent transcription by altering the histone acetyltransferases activity of coactivators p300 and PCAF (7). In an HSV-1-infected cell, the viral immediate-early genes trigger the loss of TFIIE, leading to aberrant phosphorylation of the RNA polymerase II large subunit and repression of host gene transcription (25). RVFV nonstructural proteins target TFIIH to achieve a drastic suppression of host cell RNA synthesis (33). In these cases, the interference of virus infection with host cell gene expression is negative. This is also a striking characteristic of the present system, in which 93 to 95% of affected genes were down-regulated, with 2.5- and 2.0-fold changes, respectively. It was reported that NS1, in particular, interferes with the phosphorylation of specific cellular proteins (1), which could represent one of the possible ways by which NS1 modulates cellular protein functioning. The molecular analysis of the impact of H-1 virus infection on the pattern of protein association with target promoters and on the alterations of components of the transcription machinery should help to unravel the interference of parvoviruses with cellular gene expression.

In summary, this study led us to identify cellular genes whose expression is altered at the mRNA level at early times in the course of parvovirus infection. Irrespective of the underlying mechanisms, our data show that most of these genes are repressed, whereas only a few are induced under natural infection. The microarray methodology therefore provides an early molecular signature of cell intoxication prior to the appearance of macroscopically or microscopically visible cellular disturbances. In all likelihood, at least some of the observed changes in cellular gene expression have a direct impact on further progress of the viral life cycle, including the later appearance of cytopathic effects. A challenge for future investigations will be to distinguish among the panel of detected changes the side effects from gene expression alterations that are actually relevant to virus replication and cytotoxicity. The use of related virus strains differing in their cytopathic potential and of cell variants differing in their sensitivity to parvovirus infection should help to narrow down the list of candidates to be tested further at the functional level for their direct implication in parvovirus-host cell interactions.

ACKNOWLEDGMENTS

We thank C. Dinsart, N. Salomé, D. Su, and J. Nüesch for critical reading of the manuscript and N. Jauniaux for his assistance in editing the figures. We also thank B. Leuchs for preparing wild-type H-1 virus and helpful discussion, N. Winkelhöfer for her help in Western blot

analysis, and M. Klein for her help in immunofluorescence analysis. We are grateful to H. Zentgraf for electron microscopy analysis of viral particles.

J. Li was supported by a predoctoral fellowship of the Service de coopération scientifique de l'Ambassade de France en Chine and is the recipient of a Deutsches Krebsforschungszentrum postdoctoral fellowship.

REFERENCES

1. **Anouja, F., R. Wattiez, S. Mousset, and P. Caillet-Fauquet.** 1997. The cytotoxicity of the parvovirus minute virus of mice nonstructural protein NS1 is related to changes in the synthesis and phosphorylation of cell proteins. J. Virol. **71:**4671–4678.
2. **Bashir, T., R. Hörlein, J. Rommelaere, and K. Willwand.** 2000. Cyclin A activates the DNA polymerase δ-dependent elongation machinery in vitro: a parvovirus DNA replication model. Proc. Natl. Acad. Sci. USA **97:**5522–5527.
3. **Bodendorf, U., C. Cziepluch, J. C. Jauniaux, J. Rommelaere, and N. Salomé.** 1999. Nuclear export factor CRM1 interacts with nonstructural proteins NS2 from parvovirus minute virus of mice. J. Virol. **73:**7769–7779.
4. **Brandenburger, A., D. Legendre, B. Avalosse, and J. Rommelaere.** 1990. NS-1 and NS-2 proteins may act synergistically in the cytopathogenicity of parvovirus MVMp. Virology **174:**576–584.
5. **Brockhaus, K., S. Plaza, D. J. Pintel, J. Rommelaere, and N. Salomé.** 1996. Nonstructural proteins NS2 of minute virus of mice associate in vivo with 14-3-3 protein family members. J. Virol. **70:**7527–7534.
6. **Caillet-Fauquet, P., M. Perros, A. Brandenburger, P. Spegelaere, and J. Rommelaere.** 1990. Programmed killing of human cells by means of an inducible clone of parvoviral genes encoding non-structural proteins. EMBO J. **9:**2989–2995.
7. **Chakravarti, D., V. Ogryzko, H. Y. Kao, A. Nash, H. Chen, Y. Nakatani, and R. M. Evans.** 1999. A viral mechanism for inhibition of p300 and PCAF acetyltransferase activity. Cell **96:**393–403.
8. **Christensen, J., S. F. Cotmore, and P. Tattersall.** 1997. Parvovirus initiation factor PIF: a novel human DNA-binding factor which coordinately recognizes two ACGT motifs. J. Virol. **71:**5733–5741.
9. **Cornelis, J. J., N. Salomé, C. Dinsart, and J. Rommelaere.** 2004. Vectors based on autonomous parvoviruses: novel tools to treat cancer? J. Gene Med. **6**(Suppl. 1)**:**S193–S202.
10. **Cotmore, S. F., J. Christensen, J. P. Nuesch, and P. Tattersall.** 1995. The NS1 polypeptide of the murine parvovirus minute virus of mice binds to DNA sequences containing the motif [ACCA]2–3. J. Virol. **69:**1652–1660.
11. **Cotmore, S. F., A. M. D'Abramo, Jr., L. F. Carbonell, J. Bratton, and P. Tattersall.** 1997. The NS2 polypeptide of parvovirus MVM is required for capsid assembly in murine cells. Virology **231:**267–280.
12. **Cotmore, S. F., and P. Tattersall.** 1987. The autonomously replicating parvoviruses of vertebrates. Adv. Virus Res. **33:**91–174.
13. **Cziepluch, C., E. Kordes, R. Poirey, A. Grewenig, J. Rommelaere, and J. C. Jauniaux.** 1998. Identification of a novel cellular TPR-containing protein, SGT, that interacts with the nonstructural protein NS1 of parvovirus H-1. J. Virol. **72:**4149–4156.
14. **Dai, Y., B. Gold, J. K. Vishwanatha, and S. L. Rhode.** 1994. Mimosine inhibits viral DNA synthesis through ribonucleotide reductase. Virology **205:**210–216.
15. **Deleu, L., F. Fuks, D. Spitkovsky, R. Hörlein, S. Faisst, and J. Rommelaere.** 1998. Opposite transcriptional effects of cyclic AMP-responsive elements in confluent or $p27^{KIP}$-overexpressing cells versus serum-starved or growing cells. Mol. Cell. Biol. **18:**409–419.
16. **Eichwald, V., L. Daeffler, M. Klein, J. Rommelaere, and N. Salomé.** 2002. The NS2 proteins of parvovirus minute virus of mice are required for efficient nuclear egress of progeny virions in mouse cells. J. Virol. **76:**10307–10319.
17. **Everett, H., and G. McFadden.** 1999. Apoptosis: an innate immune response to virus infection. Trends Microbiol. **7:**160–165.
18. **Faisst, S. R., S. Faisst, C. Grangette, J. R. Schlehofer, and J. Rommelaere.** 1993. NFκB upstream regulatory sequences of the HIV-1 LTR are involved in the inhibition of HIV-1 promoter activity by the NS proteins of autonomous parvoviruses H-1 and MVMp. Virology **197:**770–773.
19. **Fuks, F., L. Deleu, C. Dinsart, J. Rommelaere, and S. Faisst.** 1996. *ras* oncogene-dependent activation of the P4 promoter of minute virus of mice through a proximal P4 element interacting with the Ets family of transcription factors. J. Virol. **70:**1331–1339.
20. **Granville, D. J., C. M. Carthy, D. Yang, D. W. Hunt, and B. M. McManus.** 1998. Interaction of viral proteins with host cell death machinery. Cell Death Differ. **5:**653–659.
21. **Guo, L., G. Li, H. Xu, W. Lin, H. Huang, Z. Luo, and Z. Su.** 1999. p53 gene expression of human hepatoma cell lines and their sensitivities to parvovirus H-1. Shi Yan Sheng Wu Xue Bao **32:**23–29.
22. **Hardt, N., C. Dinsart, S. Spadari, G. Pedrali-Noy, and J. Rommelaere.** 1983. Interrelation between viral and cellular DNA synthesis in mouse cells infected with the parvovirus minute virus of mice. J. Gen. Virol. **64:**1991–1998.
23. **Harris, A. L.** 2002. Hypoxia–a key regulatory factor in tumour growth. Nat. Rev. Cancer **2:**38–47.
24. **Jain, M., C. Arvanitis, K. Chu, W. Dewey, E. Leonhardt, M. Trinh, C. D. Sundberg, J. M. Bishop, and D. W. Felsher.** 2002. Sustained loss of a neoplastic phenotype by brief inactivation of MYC. Science **297:**102–104.
25. **Jenkins, H. L., and C. A. Spencer.** 2001. RNA polymerase II holoenzyme modifications accompany transcription reprogramming in herpes simplex virus type 1-infected cells. J. Virol. **75:**9872–9884.
26. **Kestler, J., B. Neeb, S. Struyf, J. Van Damme, S. F. Cotmore, A. D'Abramo, P. Tattersall, J. Rommelaere, C. Dinsart, and J. J. Cornelis.** 1999. *cis* requirements for the efficient production of recombinant DNA vectors based on autonomous parvoviruses. Hum. Gene Ther. **10:**1619–1632.
27. **Krady, J. K., and D. C. Ward.** 1995. Transcriptional activation by the parvoviral nonstructural protein NS-1 is mediated via a direct interaction with Sp1. Mol. Cell. Biol. **15:**524–533.
28. **Lachmann, S., J. Rommeleare, and J. P. F. Nüesch.** 2003. Novel PKCη is required to activate replicative functions of the major nonstructural protein NS1 of minute virus of mice. J. Virol. **77:**8048–8060.
29. **Lalande, M.** 1990. A reversible arrest point in the late G_1 phase of the mammalian cell cycle. Exp. Cell Res. **186:**332–339.
30. **Lang, S.** 2003. Ph.D. thesis. Universität Heidelberg, Heidelberg, Germany. [Online.] http://www.ub.uni-heidelberg.de/archiv/3380.
31. **Legendre, D., and J. Rommelaere.** 1992. Terminal regions of the NS-1 protein of the parvovirus minute virus of mice are involved in cytotoxicity and promoter *trans* inhibition. J. Virol. **66:**5705–5713.
32. **Legrand, C., J. Rommelaere, and P. Caillet-Fauquet.** 1993. MVM(p) NS-2 protein expression is required with NS-1 for maximal cytotoxicity in human transformed cells. Virology **195:**149–155.
33. **Le May, N., S. Dubaele, L. P. De Santis, A. Billecocq, M. Bouloy, and J. M. Egly.** 2004. TFIIH transcription factor, a target for the Rift Valley hemorrhagic fever virus. Cell **116:**541–550.
34. **Leung, D. W., G. Cachianes, W. J. Kuang, D. V. Goeddel, and N. Ferrara.** 1989. Vascular endothelial growth factor is a secreted angiogenic mitogen. Science **246:**1306–1309.
35. **Lopez-Guerrero, J. A., B. Rayet, M. Tuynder, J. Rommelaere, and C. Dinsart.** 1997. Constitutive activation of U937 promonocytic cell clones selected for their resistance to parvovirus H-1 infection. Blood **89:**1642–1653.
36. **Lorson, C., J. Pearson, L. Burger, and D. J. Pintel.** 1998. An Sp1-binding site and TATA element are sufficient to support full transactivation by proximally bound NS1 protein of minute virus of mice. Virology **240:**326–337.
37. **Mechta-Grigoriou, F., D. Gerald, and M. Yaniv.** 2001. The mammalian Jun proteins: redundancy and specificity. Oncogene **20:**2378–2389.
38. **Merola, M., B. Blanchard, and M. G. Tovey.** 1996. The kappa B enhancer of the human interleukin-6 promoter is necessary and sufficient to confer an IL-1 beta and TNF-alpha response in transfected human cell lines: requirement for members of the C/EBP family for activity. J. Interferon Cytokine Res. **16:**783–798.
39. **Miao, L., P. Yi, Y. Wang, and M. Wu.** 2003. Etoposide upregulates Bax-enhancing tumour necrosis factor-related apoptosis inducing ligand-mediated apoptosis in the human hepatocellular carcinoma cell line QGY-7703. Eur. J. Biochem. **270:**2721–2731.
40. **Moehler, M., B. Blechacz, N. Weiskopf, M. Zeidler, W. Stremmel, J. Rommelaere, P. R. Galle, and J. J. Cornelis.** 2001. Effective infection, apoptotic cell killing and gene transfer of human hepatoma cells but not primary hepatocytes by parvovirus H1 and derived vectors. Cancer Gene Ther. **8:**158–167.
41. **Moehler, M., M. Zeidler, J. Schede, J. Rommelaere, P. R. Galle, J. J. Cornelis, and M. Heike.** 2003. Oncolytic parvovirus H1 induces release of heat-shock protein HSP72 in susceptible human tumor cells but may not affect primary immune cells. Cancer Gene Ther. **10:**477–480.
42. **Mousset, S., Y. Ouadrhiri, P. Caillet-Fauquet, and J. Rommelaere.** 1994. The cytotoxicity of the autonomous parvovirus minute virus of mice nonstructural proteins in FR3T3 rat cells depends on oncogene expression. J. Virol. **68:**6446–6453.
43. **Norton, J. D., and G. T. Atherton.** 1998. Coupling of cell growth control and apoptosis functions of Id proteins. Mol. Cell. Biol. **18:**2371–2381.
44. **Nüesch, J. P., S. F. Cotmore, and P. Tattersall.** 1995. Sequence motifs in the replicator protein of parvovirus MVM essential for nicking and covalent attachment to the viral origin: identification of the linking tyrosine. Virology **209:**122–135.
45. **Nüesch, J. P., S. Lachmann, R. Corbau, and J. Rommelaere.** 2003. Regulation of minute virus of mice NS1 replicative functions by atypical PKCλ in vivo. J. Virol. **77:**433–442.
46. **Oehler, M. K., C. Norbury, S. Hague, M. C. Rees, and R. Bicknell.** 2001. Adrenomedullin inhibits hypoxic cell death by upregulation of Bcl-2 in endometrial cancer cells: a possible promotion mechanism for tumour growth. Oncogene **20:**2937–2945.
47. **Ohshima, T., E. Yoshida, T. Nakajima, K. I. Yagami, and A. Fukamizu.** 2001. Effects of interaction between parvovirus minute virus of mice NS1 and coactivator CBP on NS1- and p53-transactivation. Int. J. Mol. Med. **7:**49–54.
48. **Op De Beeck, A., J. Sobczak-Thepot, H. Sirma, F. Bourgain, C. Brechot, and**

P. Caillet-Fauquet. 2001. NS1- and minute virus of mice-induced cell cycle arrest: involvement of p53 and $p21^{cip1}$. J. Virol. **75:**11071–11078.
49. **Pelengaris, S., M. Khan, and G. Evan.** 2002. c-MYC: more than just a matter of life and death. Nat. Rev. Cancer **2:**764–776.
50. **Perros, M., L. Deleu, J.-M. Vanacker, Z. Kherrouche, N. Spruyt, S. Faisst, and J. Rommelaere.** 1995. Upstream CREs participate in the basal activity of minute virus of mice promoter P4 and in its stimulation in *ras*-transformed cells. J. Virol. **69:**5506–5515.
51. **Pitti, R. M., S. A. Marsters, D. A. Lawrence, M. Roy, F. C. Kischkel, P. Dowd, A. Huang, C. J. Donahue, S. W. Sherwood, D. T. Baldwin, P. J. Godowski, W. I. Wood, A. L. Gurney, K. J. Hillan, R. L. Cohen, A. D. Goddard, D. Botstein, and A. Ashkenazi.** 1998. Genomic amplification of a decoy receptor for Fas ligand in lung and colon cancer. Nature **396:**699–703.
52. **Rayet, B., J.-A. Lopez-Guerrero, J. Rommelaere, and C. Dinsart.** 1998. Induction of programmed cell death by parvovirus H-1 in U937 cells: connection with the tumor necrosis factor alpha signalling pathway. J. Virol. **72:**8893–8903.
53. **Rhode, S. L., III.** 1973. Replication process of the parvovirus H-1. I. Kinetics in a parasynchronous cell system. J. Virol. **11:**856–861.
54. **Rhode, S. L., III, and S. M. Richard.** 1987. Characterization of the *trans*-activation-responsive element of the parvovirus H-1 P38 promoter. J. Virol. **61:**2807–2815.
55. **Rommelaere, J., and J. J. Cornelis.** 1991. Antineoplastic activity of parvoviruses. J. Virol. Methods **33:**233–251.
56. **Salomé, N., B. van Hille, N. Duponchel, G. Meneguzzi, F. Cuzin, J. Rommelaere, and J. J. Cornelis.** 1990. Sensitization of transformed rat cells to parvovirus MVMp is restricted to specific oncogenes. Oncogene **5:**123–130.
57. **Schlehofer, J. R., M. Rentrop, and D. N. Mannel.** 1992. Parvoviruses are inefficient in inducing interferon-beta, tumor necrosis factor-alpha, or interleukin-6 in mammalian cells. Med. Microbiol. Immunol. **181:**153–164.
58. **Shi, Z. Y., C. W. Ma, J. Huang, W. M. Lin, R. C. Dong, and Z. Y. Luo.** 1997. Inhibition of parvovirus H-1 on transplantable human hepatoma and its histological and histobiochemical studies. Shi Yan Sheng Wu Xue Bao **30:** 247–259.
59. **Shoshani, T., A. Faerman, I. Mett, E. Zelin, T. Tenne, S. Gorodin, Y. Moshel, S. Elbaz, A. Budanov, A. Chajut, H. Kalinski, I. Kamer, A. Rozen, O. Mor, E. Keshet, D. Leshkowitz, P. Einat, R. Skaliter, and E. Feinstein.** 2002. Identification of a novel hypoxia-inducible factor 1-responsive gene, RTP801, involved in apoptosis. Mol. Cell. Biol. **22:**2283–2293.
60. **Siegl, G., and M. Gautschi.** 1973. The multiplication of parvovirus Lu3 in a synchronized culture system. II. Biochemical characteristics of virus replication. Arch. Gesamte Virusforsch. **40:**119–127.
61. **Soldani, C., and A. I. Scovassi.** 2002. Poly(ADP-ribose) polymerase-1 cleavage during apoptosis: an update. Apoptosis **7:**321–328.
62. **Song, L., A. Mercado, N. Vazquez, Q. Xie, R. Desai, A. L. George, Jr., G. Gamba, and D. B. Mount.** 2002. Molecular, functional, and genomic characterization of human KCC2, the neuronal K-Cl cotransporter. Brain Res. Mol. Brain Res. **103:**91–105.
63. **Staller, P., J. Sulitkova, J. Lisztwan, H. Moch, E. J. Oakeley, and W. Krek.** 2003. Chemokine receptor CXCR4 downregulated by von Hippel-Lindau tumour suppressor pVHL. Nature **425:**307–311.
64. **Stilwell, J. L., and R. J. Samulski.** 2004. Role of viral vectors and virion shells in cellular gene expression. Mol. Ther. **9:**337–346.
65. **Su, Z. Z., Z. Y. Luo, L. P. Guo, J. Z. Li, and Y. L. Liu.** 1988. Inhibitory effect of parvovirus H-1 on cultured human tumour cells or transformed cells. Sci. Sin. Ser. B **31:**69–80.
66. **Tattersall, P., and J. Bratton.** 1983. Reciprocal productive and restrictive virus-cell interactions of immunosuppressive and prototype strains of minute virus of mice. J. Virol. **46:**944–955.
67. **Vanacker, J.-M., R. Corbau, G. Adelmant, M. Perros, V. Laudet, and J. Rommelaere.** 1996. Transactivation of a cellular promoter by the NS1 protein of the parvovirus minute virus of mice through a putative hormone-responsive element. J. Virol. **70:**2369–2377.
68. **Volpert, O. V., R. Pili, H. A. Sikder, T. Nelius, T. Zaichuk, C. Morris, C. B. Shiflett, M. K. Devlin, K. Conant, and R. M. Alani.** 2002. Id1 regulates angiogenesis through transcriptional repression of thrombospondin-1. Cancer Cell. **2:**473–483.
69. **Wilson, G. M., H. K. Jindal, D. E. Yeung, W. Chen, and C. R. Astell.** 1991. Expression of minute virus of mice major nonstructural protein in insect cells: purification and identification of ATPase and helicase activities. Virology **185:**90–98.
70. **Wrzesinski, C., L. Tesfay, N. Salomé, J. C. Jauniaux, J. Rommelaere, J. Cornelis, and C. Dinsart.** 2003. Chimeric and pseudotyped parvoviruses minimize the contamination of recombinant stocks with replication-competent viruses and identify a DNA sequence that restricts parvovirus H-1 in mouse cells. J. Virol. **77:**3851–3858.
71. **Yan, S., C. Ma, X. Chen, S. Wan, and Z. Luo.** 1994. Inhibitory effect of parvovirus H-1 on the formation of colonies of human hepatoma cell line in vitro and its tumours in nude mice. Cell Res. **4:**47–56.
72. **Young, P. J., K. T. Jensen, L. R. Burger, D. J. Pintel, and C. L. Lorson.** 2002. Minute virus of mice NS1 interacts with the SMN protein, and they colocalize in novel nuclear bodies induced by parvovirus infection. J. Virol. **76:**3892–3904.
73. **Zhang, H., Y. Ramanathan, P. Soteropoulos, M. L. Recce, and P. P. Tolias.** 2002. EZ-Retrieve: a web-server for batch retrieval of coordinate-specified human DNA sequences and underscoring putative transcription factor-binding sites. Nucleic Acids Res. **30:**E121.